ACTA CHEMICA SCANDINAVICA 21 (1967) 527–536

On the Solid Solubility and Structural Properties of $PdAs_{2-x}Sb_x$, $PtP_{2-x}As_x$, $PtP_{2-x}Sb_x$, $PtP_{2-x}Bi_x$, $PtAs_{2-x}Sb_x$, $PtAs_{2-x}Bi_x$, $PtSb_{2-x}Bi_x$, $Pd_{1-m}Pt_mAs_2$, $Pd_{1-m}Pt_mSb_2$, $Pd_{1-m}Au_mSb_2$, and $Pt_{1-m}Au_mSb_2$

SIGRID FURUSETH, KARI SELTE and ARNE KJEKSHUS

Kjemisk Institutt A, Universitetet i Oslo, Blindern, Oslo 3, Norway

The mutual solid solubilities of the compounds $PdAs_2$, $PdSb_2$, PtP_2, $PtAs_2$, $PtSb_2$, α-$PtBi_2$, and $AuSb_2$ with pyrite type crystal structure have been investigated by the X-ray powder method. Complete solid solution ranges from $x = 0.00$ to $x = 2.00$ are observed for $PdAs_{2-x}Sb_x$, $PtP_{2-x}As_x$, and $PtSb_{2-x}Bi_x$, limited solid solubility is found for $PtAs_{2-x}Sb_x$ ($0.00 \leqq x \leqq 0.2$ and $1.3 < x \leqq 2.00$ at 1000°C) and $Pd_{1-m}Au_mSb_2$ ($0.00 \leqq m \leqq 0.25$ at 600°C), and no solid solubility is detected for $PtP_{2-x}Sb_x$, $PtP_{2-x}Bi_x$, $PtAs_{2-x}Bi_x$, $Pd_{1-m}Pt_mAs_2$, $Pd_{1-m}Pt_mSb_2$, and $Pt_{1-m}Au_mSb_2$. The results are discussed in relation to the relative sizes of the substituting atoms and the crystallographic features of the pyrite type crystal structure.

Among the binary di-pnictides of the sub-group elements, seven are known to crystallize with the pyrite type crystal structure, *i.e.* $PdAs_2$, $PdSb_2$, PtP_2, $PtAs_2$, $PtSb_2$, α-$PtBi_2$, and $AuSb_2$. A redetermination of the crystal structures of these compounds has recently been reported by the present authors [1] and structural data from that paper are quoted in Table 1. (For

Table 1. Structural data for $PdAs_2$, $PdSb_2$, PtP_2, $PtAs_2$, $PtSb_2$, α-$PtBi_2$, and $AuSb_2$.

Compound	a (Å)	u	M-X distance (Å)	X-X distance (Å)
$PdAs_2$	5.9855 ± 0.0005	0.383 ± 0.001	2.498 ± 0.002	2.42_6 ± 0.02
$PdSb_2$	6.4584 ± 0.0005	0.371 ± 0.002	2.671 ± 0.004	2.88_6 ± 0.05
PtP_2	5.6956 ± 0.0005	0.394 ± 0.004	2.401 ± 0.010	2.09_1 ± 0.08
$PtAs_2$	5.9665 ± 0.0004	0.383 ± 0.002	2.490 ± 0.004	2.41_8 ± 0.04
$PtSb_2$	6.4400 ± 0.0004	0.375 ± 0.002	2.669 ± 0.004	2.78_9 ± 0.05
α-$PtBi_2$	6.7022 ± 0.0006	0.371 ± 0.002	2.771 ± 0.004	2.99_5 ± 0.05
$AuSb_2$	6.6583 ± 0.0005	0.376 ± 0.002	2.763 ± 0.004	2.86_0 ± 0.05

further information concerning structural, magnetic, and electrical properties of the compounds, see Refs. 2—23.)

The present study was carried out with the purpose of investigating the mutual exchange of two metals, or two pnigogen elements, in these phases, *i.e.* the preparation of ternary phases obeying the formulae $M^1_{1-m}M^2_mX_2$ $(0 < m < 1)$ and $MX^1_{2-x}X^2_x$ $(0 < x < 2)$. (In these formulae M indicates Pd, Pt, or Au, and X denotes P, As, Sb, or Bi.) Our investigation was initiated by a paper by Hulliger,[11] where, *inter alia*, the existence, unit cell dimensions, and electrical and magnetic properties of the "compounds" PdAsSb, PtPAs, and PtSbBi are reported. Hulliger gives the impression that there exist three distinct "compounds", whereas in our opinion there is no other significance to be attached to his formulae than that exactly 50 atomic % of X^1 has been substituted by X^2.

EXPERIMENTAL

The samples were prepared from 99.999 % Pd and Pt (L. Light & Co., Ltd. or Johnson, Matthey & Co., Ltd.), 99.995 % Au (L. Light & Co., Ltd.), 99.999 % red P (Koch-Light Laboratories, Ltd.), 99.999 + % As and Sb (Johnson, Matthey & Co., Ltd.), and 99.99 + % Bi (American Smelting and Refining Co.) by heating weighed quantities of the powdered components in evacuated and sealed silica tubes. Several samples (in most of the systems) were also made from weighed amounts of the binary compounds $PdAs_2$, $PdSb_2$, PtP_2, $PtAs_2$, $PtSb_2$, α-$PtBi_2$, and $AuSb_2$. (The binary compounds had previously been synthesized at 600°C.) In most cases crucibles of pure alumina were placed inside the silica tubes to avoid reactions between the samples and SiO_2. The heat treatments used in the various systems are recorded in Table 2.

Table 2. Heat treatment used in sample preparation. The following abbreviations are used: d (annealing period in days), s (slowly cooled), q (quenched in ice water).

t (°C)	600	700	800	1000	1200
$PdAs_{2-x}Sb_x$	60 d (s)	14 d (q)			
$PtP_{2-x}As_x$	60 d (s)	14 d (q)		1 d (s,q)	
$PtAs_{2-x}Sb_x$	60 d (s)	14 d (q)	7 d (q)	1 d (q), 2 d (s)	1 d (q)
$PtSb_{2-x}Bi_x$	60 d (s)	14 d (q)			
$PtP_{2-x}Sb_x$	14 d (s)			1 d (q,s)	
$PtP_{2-x}Bi_x$	14 d (s)			1 d (q,s)	
$PtAs_{2-x}Bi_x$	14 d (s)			1 d (q,s)	
$Pd_{1-m}Au_mSb_2$	14 d (s)			1 d (q)	
$Pd_{1-m}Pt_mAs_2$	60 d (s)			1 d (q,s)	1 d (q)
$Pd_{1-m}Pt_mSb_2$	60 d (s)			1 d (q,s)	1 d (q)
$Pt_{1-m}Au_mSb_2$	60 d (s)			1 d (q,s)	1 d (q)

A variety of samples of different compositions were prepared in each system. However, a considerable number of useless samples were made during this study resulting from great difficulties in obtaining true equilibrium, and the results presented in the succeeding section correspond only to a small fraction of the samples prepared.

All samples were crushed and X-ray photographs taken in a Guinier type focusing camera of 80 mm diameter, using strictly monochromatized Cu$K\alpha_1$-radiation. Potassium chloride (Analar, The British Drug Houses Ltd., $a = 6.2919$ Å [24]) was added to the

specimen as an internal standard. The lattice constants are expressed in Ångström units on the basis of $\lambda(\mathrm{Cu}K\alpha_1) = 1.54050$ Å. The probable error in the lattice constant determinations is estimated to be about ± 0.001 Å.

RESULTS

The X-ray powder (Guinier) photographs were composed of sharp reflections for all samples prepared in this study. (An exception however, must be made in the case of some of the samples belonging to the system $Pd_{1-m}Au_mSb_2$; see below.) The diffraction patterns could be indexed assuming the presence of either one or two phases of cubic symmetry in the samples, and the deduced unit cell dimensions (a) resemble those found for the corresponding binary compounds. Tentative intensity calculations based on a pyrite type crystal structure were carried out for the systems where solid solubility has been observed. A comparison of the observed and calculated intensities of the reflections on the Guinier photographs confirmed the proposed structure with u-parameters of the same size as found for the binary compounds. However, the observed data do not allow a detailed refinement of the u-parameters. It should be emphasized that failure to observe additional superstructure reflections on the Guinier photographs shows that the substituted atoms are arranged at random in the M or X sublattices.

Examples of complete, limited, and no solid solubility have been observed in the various systems.

The systems $PdAs_{2-x}Sb_x$, $PtP_{2-x}As_x$, and $PtSb_{2-x}Bi_x$. Complete solid solution ranges from $x = 0.00$ to $x = 2.00$ have been found for $PdAs_{2-x}Sb_x$, $PtP_{2-x}As_x$, and $PtSb_{2-x}Bi_x$, with continuous variations in the unit cell dimensions as functions of composition (Figs. 1—3). Essentially linear relationships between a and x are observed for $PtP_{2-x}As_x$ and $PtSb_{2-x}Bi_x$, whereas a systematic deviation from the linear dependence is noticed for $PdAs_{2-x}Sb_x$.

The lattice dimensions of PdAsSb, PtPAs, and PtSbBi reported by Hulliger [11] are included in Figs. 1—3 for the purpose of comparison. Hulliger's data show good agreement with those obtained in this study for PtPAs and PtSbBi, whereas his a-value for PdAsSb is somewhat different from the present one.

Equilibrium in the systems $PdAs_{2-x}Sb_x$ and $PtSb_{2-x}Bi_x$ was easily attained at 600°C using the pure elements as starting materials. In the system $PtP_{2-x}As_x$, however, equilibrium was only obtained at a temperature of 1000°C, and preparations starting from PtP_2 and $PtAs_2$ gave the best results.

The system $PtAs_{2-x}Sb_x$. The present results indicate that $PtAs_2$ and $PtSb_2$ are only partially soluble in each other at temperatures between 600 and 1200°C. The diagram of Fig. 4 refers to a preparation temperature of 1000°C, at which substitutional solid solution is observed within the regions $0.00 \leqq x \leqq 0.2$ and $1.3 < x \leqq 2.00$. The Guinier photographic data collected for samples quenched from 1200°C suggest very strongly that the homogeneity ranges may be somewhat extended ($0.00 \leqq x < \sim 0.3$ and $\sim 1.0 < x \leqq 2.00$ at 1200°C). Complete solid solubility may even occur at still higher temperatures. Considerable difficulties associated with the quenching procedure prevent us from giving a definite experimental answer at this stage.

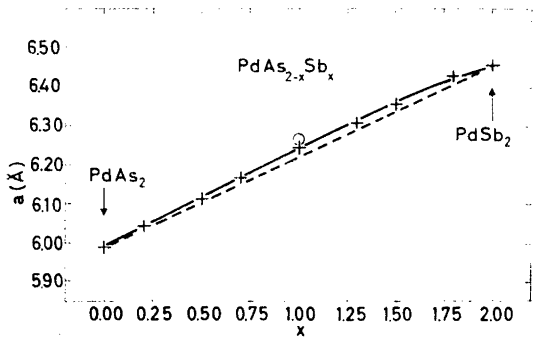

Fig. 1. Lattice constants of $PdAs_{2-x}Sb_x$ as a function of composition. The lattice constant reported by Hulliger[11] (O) for $x = 1$ is indicated. The broken line shows the Vegard law relationship and the solid curve is calculated from the combination of eqns. 5, 6, 7, 9, and 11 using the numerical data of Table 1 (see text).

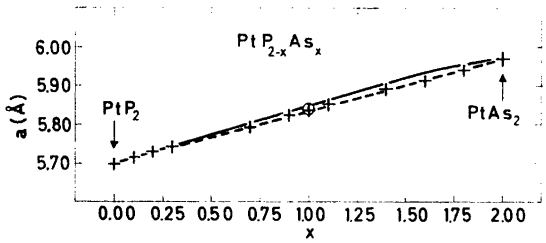

Fig. 2. Lattice constants *versus* composition relationship for $PtP_{2-x}As_x$. (See caption to Fig. 1.)

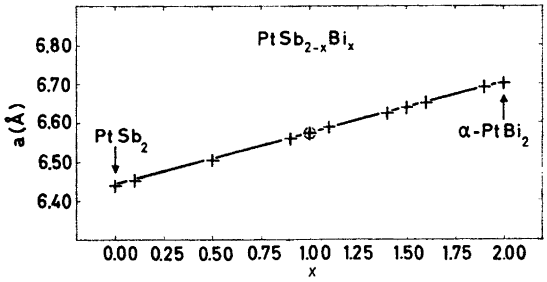

Fig. 3. Lattice constants as a function of composition for $PtSb_{2-x}Bi_x$. (See caption to Fig. 1.)

Equilibrium in the $PtAs_{2-x}Sb_x$ system was most easily obtained by heating mixed powders of $PtAs_2$ and $PtSb_2$.

The system $Pd_{1-m}Au_mSb_2$. Limited solid solubility has been found for $Pd_{1-m}Au_mSb_2$ in the range $0.00 \leq m \leq 0.25$ (600°C), *cf.* Fig. 5. It is remarkable that Pd is not interchangeable with the Au in $AuSb_2$ (Pd having a smaller size than Au), while there is appreciable substitution of Pd by Au in $PdSb_2$.

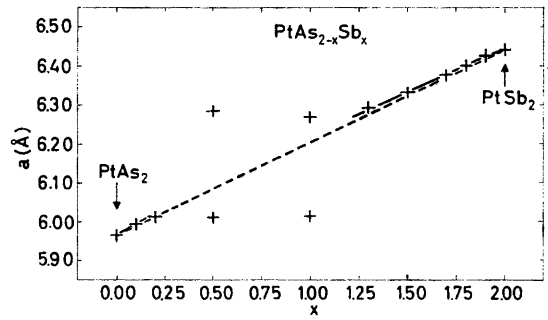

Fig. 4. Lattice constants *versus* composition relationship for $PtAs_{2-x}Sb_x$. (See caption to Fig. 1.)

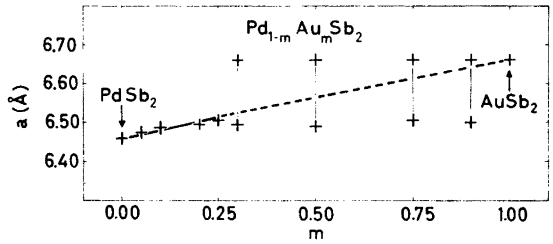

Fig. 5. Lattice constants of $Pd_{1-m}Au_mSb_2$ as a function of composition. (See caption to Fig. 1 and text.)

The diffraction patterns of samples in the two-phase region of the $Pd_{1-m}Au_mSb_2$ system (most striking for samples synthesized at 600°C) differ markedly in one respect from those obtained in the other systems. For samples with $0.3 \leqq m \leqq 0.9$ shaded regions (indicated by the faint vertical lines in Fig. 5) of distinct blackening on the Guinier photographs are easily visible between the sharp reflections corresponding to $Pd_{0.75}Au_{0.25}Sb_2$ and $AuSb_2$. This observation suggests that the equilibrium conditions in the $Pd_{1-m}Au_mSb_2$ system may be governed by kinetic effects rather than by thermodynamics. It indicates furthermore that complete solid solubility may be obtained in this system by protracted annealing at low temperatures ($\leqq$ 600°C).

The systems $PtP_{2-x}Sb_x$, $PtP_{2-x}Bi_x$, $PtAs_{2-x}Bi_x$, $Pd_{1-m}Pt_mAs_2$, $Pd_{1-m}Pt_mSb_2$, *and* $Pt_{1-m}Au_mSb_2$. All samples prepared in the systems $PtP_{2-x}Sb_x$, $PtP_{2-x}Bi_x$, $PtAs_{2-x}Bi_x$, $Pd_{1-m}Pt_mAs_2$, $Pd_{1-m}Pt_mSb_2$, and $Pt_{1-m}Au_mSb_2$ with $0 < x < 2$ or $0 < m < 1$ proved to contain a mixture of the two corresponding binary compounds. For each of these systems the deduced lattice dimensions agreed within the error limits with those of the pure MX_2 compounds, regardless of the nominal compositions of the samples. It is accordingly concluded that no indication of solid solubility is observed in any of these systems. However, it should be mentioned that the unit cell dimensions of $PdAs_2$ and $PdSb_2$ are almost equal to those of $PtAs_2$ and $PtSb_2$, respectively. Thus, even a solubility

of up to 10 atomic % Pd with Pt, and *vice versa*, in the systems $Pd_{1-m}Pt_mAs_2$ and $Pd_{1-m}Pt_mSb_2$ would hardly be noticed by examination of the Guinier photographic data.

DISCUSSION

In an attempt to correlate the present results it seems appropriate to discuss the large differences in solid solubility observed in the various systems and secondly to consider the apparent deviation from Vegard's law noticed in Fig. 1.

The empirical rule of Hume-Rothery [25] states that unless the solute and solvent radii lie within about 15 % of each other, extensive substitutional solid solutions cannot be formed even though all other controlling factors (*e.g.* the relative valences and electronegativities) are favourable. As this rule appears to be valid quite generally, radius ratios were calculated for the atom combinations in question. The following apparent radii are deduced from Table 1 (in Å; average values are estimated, when possible): $r_P = 1.05 \pm 0.04$, $r_{As} = 1.21 \pm 0.02$, $r_{Sb} = 1.42 \pm 0.03$, $r_{Bi} = 1.50 \pm 0.03$, $r_{Pd} = 1.26 \pm 0.03$, $r_{Pt} = 1.29 \pm 0.03$, and $r_{Au} = 1.33 \pm 0.03$. The corresponding radius ratios are: $r_{As}/r_P = 1.15 \pm 0.07$, $r_{Sb}/r_P = 1.35 \pm 0.09$, $r_{Bi}/r_P = 1.43 \pm 0.09$, $r_{Sb}/r_{As} = 1.17 \pm 0.05$, $r_{Bi}/r_{As} = 1.24 \pm 0.05$, $r_{Bi}/r_{Sb} = 1.06 \pm 0.05$, $r_{Pt}/r_{Pd} = 1.02 \pm 0.05$, $r_{Au}/r_{Pd} = 1.06 \pm 0.05$, and $r_{Au}/r_{Pt} = 1.03 \pm 0.05$.

Application of Hume-Rothery's rule separates the favourable ratios r_{Bi}/r_{Sb}, r_{Pt}/r_{Pd}, r_{Au}/r_{Pd}, and r_{Au}/r_{Pt} from the unfavourable combinations r_{Sb}/r_P, r_{Bi}/r_P, and r_{Bi}/r_{As}, leaving r_{As}/r_P and r_{Sb}/r_{As} as borderline cases. The negative observations for $PtP_{2-x}Sb_x$, $PtP_{2-x}Bi_x$, and $PtAs_{2-x}Bi_x$ are thus readily attributed to the size effect. The borderline case of r_{Sb}/r_{As} is nicely illustrated by the different solid solubility observed for $PdAs_{2-x}Sb_x$ and $PtAs_{2-x}Sb_x$. The necessary, but insufficient limitation implied in Hume-Rothery's rule is emphasized by the failure to detect solid solubility in the systems $Pd_{1-m}Pt_mAs_2$, $Pd_{1-m}Pt_mSb_2$, and $Pt_{1-m}Au_mSb_2$. These discrepancies may qualitatively be attributed to variations in electronic band structure, differences in charge distribution, *etc.*, but lack of data prevents a quantitative discussion.

It may be of value to mention an apparent correlation between the occurrence of solid solubility and the electrical properties (*i.e.* those closely related to the electronic band structure) of the binary compounds. (PtP_2, $PtAs_2$, and $PtSb_2$ are semiconductors and $PdAs_2$, $PdSb_2$, α-$PtBi_2$, and $AuSb_2$ are metallic conductors.[6,7,11–14,17–23]) Provided Hume-Rothery's rule is satisfied, extensive solid solubility is observed if and only if the corresponding binary compounds are electrical conductors of the same type. The continuous solid solution observed for $PtSb_{2-x}Bi_x$, *i.e.* the combination of the semiconductor $PtSb_2$ with the metallic conductor α-$PtBi_2$, is the only exception from this statement. (However, this exception may only be apparent since the energy gap in $PtSb_2$ is very small, $\Delta E = 0.07$ eV, and in α-$PtBi_2$ the conduction band might just dip into the valence band.)

The lattice constant *versus* composition diagram for $PdAs_{2-x}Sb_x$ apparently deviates from the variation predicted by Vegard's law.[26,27] The dashed straight line indicates the Vegard law relationship, and positive deviation is accord-

ingly observed in Fig. 1. Two reasons can be considered in order to account for this finding:

1) The bonding scheme is gradually modified within the solid solubility range resulting from asymmetric interactions and/or differences in the electron overlap produced by the substitution.

2) A purely crystallographic model based on atoms resembling incompressible spheres (as implicit in Vegard's law) may be sufficient to explain the observations since the variable parameter u of the pyrite type structure undergoes a variation for the binary compounds (see Table 1).

The remainder of this paper is devoted to a discussion of the deviation from Vegard's law in terms of the second explanation.

It seems appropriate to present firstly some general considerations concerning the model used to analyse the data. As a first approximation, crystals may be regarded as built of spherically symmetric atoms, with a definite radius allotted to each kind of atom, assuming furthermore that the nearest-neighbour spheres touch each other. The simplest formulation of the crystallographic additivity rule presents this model as follows: Two nearest-neighbour atoms X^1 and X^2 of spheric symmetry, separated by an interatomic distance d_{12} in the crystal can be ascribed radii r_1 and r_2 satisfying the equation

$$r_1 + r_2 = d_{12} \tag{1}$$

The atomic radius depends on the nature of the binding forces within the crystal. A classification based on atomic radii divides crystalline substances into groups (*e.g.* a coarse classification according to the ionic and covalent-metallic sets of radii, *cf.* Pauling[28]). For structures belonging to one group, the interatomic distances can be accounted for reasonably well by one set of atomic radii. Between one group and another the atomic radii may differ widely. To a higher degree of accuracy, even among structures which are commensurable, an atom cannot be assigned a characteristic, invariable radius. However, a fairly accurate and selfconsistent set of apparent radii (see above) is obtained for the binary compounds subject to this study, since the compounds belong to a group of isostructural substances with pronounced similarities in the chemical bonding.

Generally, let us consider a crystalline phase with formula $X^1_{x_1}X^2_{x_2}...X^i_{x_i}$ and assign the radius r_i to the atom X^i. If the crystallographic additivity rule is generally valid throughout its crystal lattice, *i.e.* all distances between nearest-neighbour atoms satisfy an equation similar to eqn. 1, the unit cell dimensions a_j (a_j denotes a, b, c, α, β, or γ) will obey the linear relations

$$a_j = \sum_i b_{ij} r_i \tag{2}$$

The coefficients b_{ij} of eqn. 2 depend on the composition of the phase (*i.e.* $x_1,x_2,...x_i$) and the atomic positions $u_{1k},u_{2k}, ...u_{ik}$ ($k = 1, 2, 3$) within the unit cell. (It should be noticed that the numbering of the atomic positions according to this scheme assumes that chemically equal, but crystallographically non-equivalent atoms must be counted separately.)

Eqn. 2 contains $r_1,r_2,...r_i$ as explicit variables, whereas $x_1,x_2,...x_i$ and $u_{1k},u_{2k},...u_{ik}$ enter implicitly. It is indeed possible in principle to rearrange eqn. 2 and take $x_1,x_2,...x_i$ as a new set of explicit variables, but the resulting equation will not neccessarily be linear in terms of these variables. However, under certain conditions the rearranged equation takes the form

$$a_j = \sum_i c_{ij} x_i \tag{3}$$

where the coefficients c_{ij} include $r_1,r_2,...r_i$ and $u_{1k},u_{2k},...u_{ik}$ implicitly. Eqn. 3 may be regarded as a generalized Vegard's law, since the ordinary formulation of Vegard's law follows from this expression after introduction of limitations in the concepts. These limitations consist of:

1) The effect on a_j of the reciprocal substitution of two kinds of atoms, *e.g.* X^{i-1} and X^i, is considered.

2) x_{i-1} and x_i are continuous variables satisfying the relation $x_{i-1} + x_i$ = constant, whereas $x_1, x_2, \ldots x_{i-2}$ remain fixed throughout the solid solubility range.

3) The parameters $u_{1k}, u_{2k}, \ldots u_{ik}$ specifying the atomic positions in the unit cell stay constant within the homogeneity range.

Eqn. 3 then takes the form

$$a_j = a_{0j} + c_{0j}x \tag{4}$$

where a_{0j} and c_{0j} are constants and x is a continuous variable with limited range of existence. Eqn. 4 will be recognized as the mathematical formulation of Vegard's law. (Vegard's law was originally deduced for solid solutions in ionic crystals and was later extended to metallic solid solutions.[26,27])

Let us consider a binary phase MX_2 with the pyrite type structure and express the coefficients b_M and b_X of the associated equation

$$a = b_M r_M + b_X r_X \tag{5}$$

in terms of the structural parameter u of the pyrite structure. (Except for the notations, eqn. 5 represents a simplified version of eqn. 2.) According to the construction of the pyrite type lattice (see Fig. 6) it follows that

$$b_M = 2u(3u^2 - 2u + \tfrac{1}{2})^{-\frac{1}{2}} \tag{6}$$

$$b_X = 2(3)^{-\frac{1}{2}} + 2u(3u^2 - 2u + \tfrac{1}{2})^{-\frac{1}{2}} \tag{7}$$

assuming that the crystallographic additivity model is valid.

To obtain further progress, the conceptions of effective (mean) radii r_M and r_X defined by the relations:

$$r_M = [(1 - m)r_{M^1} + mr_{M^2}] \tag{8}$$

and

$$r_X = [(2 - x)r_{X^1} + xr_{X^2}]/2 \tag{9}$$

are introduced in the model. Here r_{M^1} relates to the radius of M^1 in the corresponding binary compound M^1X_2, *etc.* It is furthermore necessary to consider the variation of the structural parameter u throughout the solid solubility range of the ternary phase. In analogy with eqns. 8 and 9 the most natural assumption seems to be to adopt the linear relations

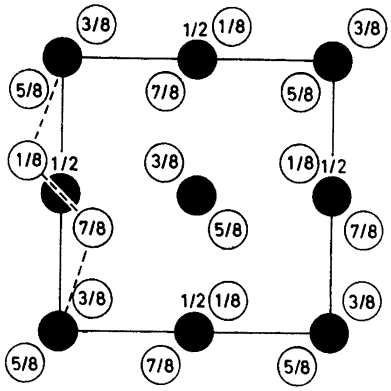

Fig. 6. The FeS_2 (pyrite) type crystal structure shown in projection. The numbers indicate fractions of the projection axis on the basis of the "ideal" atomic parameter u = 3/8. Filled and open circles represent the M and X atoms, respectively. Assuming that the crystallographic additivity model (see text) is valid, the broken lines indicate the connection between touching spheres.

$$u = [(1 - m)u_{M^1X_2} + mu_{M^2X_2}] \quad (10)$$

and

$$u = [(2 - x)u_{MX^1_2} + xu_{MX^2_2}]/2 \quad (11)$$

to define the variation of u.

Numerical calculations based on this model were carried out for the ternary phases in question, using the data for the binary phases listed in Table 1. The combination of eqns. 5, 6, 7, 8, and 10 was used for $Pd_{1-m}Au_mSb_2$ and eqns. 5, 6, 7, 9, and 11 were applied to each of the phases $PdAs_{2-x}Sb_x$, $PtP_{2-x}As_x$, $PtAs_{2-x}Sb_x$, and $PtSb_{2-x}Bi_x$. The results of these calculations are shown as the solid curves on Figs. 1—5. Significant differences between these calculated curves and the simple Vegard law relationships are only obtained for $PdAs_{2-x}Sb_x$ (Fig. 1) and $PtP_{2-x}As_x$ (Fig. 2); the two cases are discussed separately.

The close correspondence between the observed points and the calculated curves in Figs. 1, 3—5 shows that the model (*i.e.* the crystallographic additivity rule, eqns. 5—7, together with the additional specifications defined by eqns. 8—11) is sufficient to account for the observations. The apparent deviation from Vegard's law in Fig. 1 may thus be attributed to the comparatively large difference in u (see Table 1) between $PdAs_2$ and $PdSb_2$. It should be emphasized that non-linear terms are introduced in eqn. 5 by eqn. 10 or 11 in combination with eqn. 8 or 9, and that increasing differences in u increase the deviation between the dashed line and the solid curve.

The lattice constants of $PtP_{2-x}As_x$ (Fig. 2) follow the simple Vegard's law whereas the calculated curve deviates from the experimental points. This discrepancy can be accounted for by assuming $u = 0.390$ (*i.e.* lower error limit of u stated in Table 1) for PtP_2 in the calculations. Using this u-value and the associated value for r_P (1.09Å) an almost perfect coincidence between the experimental points and the calculated curve is obtained. This result together with the fact that $r_P = 1.09$ Å is a more reasonable radius for P than $r_P = 1.05$ Å suggest very strongly that the best parameter value for the PtP_2

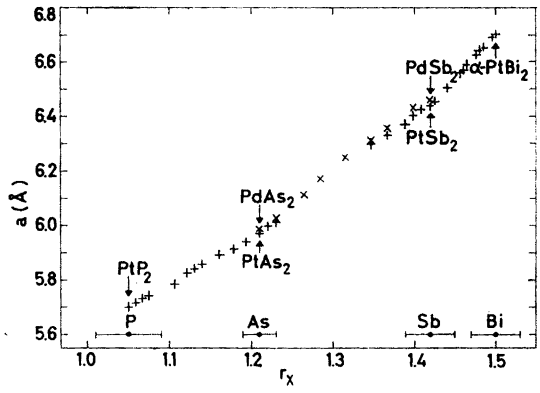

Fig. 7. Lattice constants of $PdAs_{2-x}Sb_x$, $PtP_{2-x}As_x$, $PtAs_{2-x}Sb_x$, and $PtSb_{2-x}Bi_x$ as a function of r_X (in Å. see p. 532).

structure is $u = 0.390$. (Rundqvist [10] reported $u = 0.390 \pm 0.005$, whereas $u = 0.394 \pm 0.004$ was obtained in our previous study.[1])

A compressed diagram of the results obtained for the Pd and Pt phases studied here is shown in Fig. 7, utilizing the fact that $r_{Pd} \approx r_{Pt}$. With the scale used in this diagram an essentially linear relationship between a and r_X is expected according to eqn. 5. The non-linear appearance of the diagram results mainly from the use of $r_P = 1.05$ Å. This finding is accordingly a further support for $r_P = 1.09$ Å, *i.e.* in accordance with the suggested correction of u to 0.390 for PtP_2.

REFERENCES

1. Furuseth, S., Selte, K. and Kjekshus, A. *Acta Chem. Scand.* **19** (1965) 735.
2. Oftedal, I. *Z. physik. Chem. (Leipzig)* **135** (1928) 291.
3. Thomassen, L. *Z. physik. Chem. (Leipzig)* **135** (1928) 383; **B 2** (1929) 349; **B 4** (1929) 277.
4. Wallbaum, H. J. *Z. Metallk.* **35** (1943) 200.
5. Graham, A. R. and Kaiman, S. *Am. Mineralogist* **37** (1952) 292.
6. Alekseevskii, N. E., Brandt, N. B. and Kostina, T. I. *Izv. Akad. Nauk SSSR Ser. Fiz.* **16** (1952) 233.
7. Zhuravlev, N. N. and Kertes, L. *Soviet Phys. JETP* **5** (1957) 1073.
8. Kjekshus, A. *Acta Chem. Scand.* **14** (1960) 1450.
9. Heyding, R. D. and Calvert, L. D. *Can. J. Chem.* **39** (1961) 955.
10. Rundqvist, S. *Arkiv Kemi* **20** (1962) 67.
11. Hulliger, F. *Helv. Phys. Acta* **35** (1962) 535; **37** (1964) 188; *Nature* **20** (1963) 1064.
12. Beck, A., Jan, J.-P., Pearson, W. B. and Templeton, I. M. *Phil. Mag.* **8** (1963) 351.
13. Hulliger, F. and Muller, J. *Physics Letters* **5** (1963) 226.
14. Raub, C. J. and Webb, G. W. *J. Less-Common Metals* **5** (1963) 271.
15. Raub, C. J., Zachariasen, W. H., Geballe, T. H. and Matthias, B. T. *J. Phys. Chem. Solids* **24** (1963) 1093.
16. Saini, G. S., Calvert, L. D., Heyding, R. D. and Taylor, J. B. *Can. J. Chem.* **42** (1964) 620.
17. Miller, R. C., Damon, D. H. and Sagar, A. *J. Appl. Phys.* **35** (1964) 3582.
18. Pearson, W. B. *Can. J. Phys.* **42** (1964) 519.
19. Emtage, P. R. *Phys. Rev.* **138** (1965) A246.
20. Damon, D. H., Miller, R. C. and Sagar, A. *Phys. Rev.* **138** (1965) A636.
21. Johnston, W. D., Miller, R. C. and Damon, D. H. *J. Less-Common Metals* **8** (1965) 272.
22. Hulliger, F. and Mooser, E. *J. Phys. Chem. Solids* **26** (1965) 429.
23. Fermor, J. H., Furuseth, S. and Kjekshus, A. *J. Less-Common Metals* **11** (1966) 376.
24. Hambling, P. G. *Acta Cryst.* **6** (1953) 98.
25. Hume-Rothery, W. *The Structure of Metals and Alloys*, Institute of Metals, London 1936.
26. Vegard, L. *Z. Physik* **5** (1921) 17.
27. Vegard, L. and Dale, H. *Z. Krist.* **67** (1928) 148.
28. Pauling, L. *The Nature of the Chemical Bond*, Cornell University Press, Ithaca, 1960.

Received October 31, 1966.